American Journal of Transplantation 2016; XX: 1–14
Wiley Periodicals Inc.

doi: 10.1111/ajt.14006

The Knife's Edge of Tolerance: Inducing Stable Multilineage Mixed Chimerism but With a Significant Risk of CMV Reactivation and Disease in Rhesus Macaques

H. B. Zheng[1,†], B. Watkins[2,†], V. Tkachev[1], S. Yu[3], D. Tran[3], S. Furlan[1], K. Zeleski[1], K. Singh[2], K. Hamby[2], C. Hotchkiss[4], J. Lane[4], S. Gumber[2,5], A. B. Adams[2], L. Cendales[6], A. D. Kirk[6], A. Kaur[3], B. R. Blazar[7], C. P. Larsen[2] and L. S. Kean[1,8,9,*]

[1]*Ben Towne Center for Childhood Cancer Research, Seattle Children's Research Institute, Seattle, WA*
[2]*Emory University School of Medicine, Atlanta, GA*
[3]*Tulane National Primate Research Center, New Orleans, LA*
[4]*Washington National Primate Research Center, University of Washington, Seattle, WA*
[5]*Division of Pathology, Yerkes National Primate Research Center, Emory University, Atlanta, GA*
[6]*Department of Surgery, Duke University, Durham, NC*
[7]*Department of Pediatrics, University of Minnesota, Minneapolis, MN*
[8]*Department of Pediatrics, University of Washington School of Medicine, Seattle, WA*
[9]*Fred Hutchinson Cancer Research Center, Seattle, WA*
**Corresponding author: Leslie S. Kean, leslie.kean@seattlechildrens.org*
[†]*Co-first authors.*

Although stable mixed-hematopoietic chimerism induces robust immune tolerance to solid organ allografts in mice, the translation of this strategy to large animal models and to patients has been challenging. We have previously shown that in MHC-matched nonhuman primates (NHPs), a busulfan plus combined belatacept and anti-CD154-based regimen could induce long-lived myeloid chimerism, but without T cell chimerism. In that setting, donor chimerism was eventually rejected, and tolerance to skin allografts was not achieved. Here, we describe an adaptation of this strategy, with the addition of low-dose total body irradiation to our conditioning regimen. This strategy has successfully induced multilineage hematopoietic chimerism in MHC-matched transplants that was stable for as long as 24 months posttransplant, the entire length of analysis. High-level T cell chimerism was achieved and associated with significant donor-specific prolongation of skin graft acceptance. However, we also observed significant infectious toxicities, prominently including cytomegalovirus (CMV) reactivation and end-organ disease in the setting of functional defects in anti-CMV T cell immunity. These results underscore the significant benefits that multilineage chimerism-induction approaches may represent to transplant patients as well as the inherent risks, and they emphasize the precision with which a clinically successful regimen will need to be formulated and then validated in NHP models.

Abbreviations: ALC, absolute lymphocyte count; ANC, absolute neutrophil count; ATG, antithymocyte globulin; BM, bone marrow; BMT, bone marrow transplant; BSA, body surface area; CMV, cytomegalovirus; ELISpot, enzyme-linked immunospot; G-CSF, granulocyte colony-stimulating factor; GVHD, graft-versus-host disease; HCT, hematopoietic stem cell transplant; HSC, hematopoietic stem cell; HST, honest significant difference; MGH, Massachusetts General Hospital; NHP, nonhuman primate; NIH, National Institutes of Health; TBI, total body irradiation; Tcm, central memory T cell; Tem, effector memory T cell; TLI, total lymphoid irradiation; TNC, total nucleated cell; Treg, regulatory T cell; USDA, US Department of Agriculture; WBC, white blood cell

Received 08 July 2016, revised and accepted for publication 04 August 2016

Introduction

One of the prevailing hypotheses in the field of solid organ transplantation is that if stable mixed chimerism could be reproducibly induced, then immune tolerance to both skin and solid organ allografts from the same donor would follow. In murine models, this strategy has met with widespread success (1–14). The critical importance of attaining and maintaining *multilineage* chimerism for tolerance induction has also been demonstrated in mice, where it has been shown that in the absence of T cell chimerism, tolerance induction could not be achieved (15,16). The significance of T cell chimerism to multilineage donor allogeneic hematopoietic cell chimerism stability has also been observed in clinical transplantation, where patients who lack substantial (>50–75%) donor

T cell engraftment even in the setting of significant myeloid chimerism are at high risk for loss of the donor hematopoietic graft (17–20). Although the mechanisms controlling T cell chimerism-mediated tolerance are not completely understood, they likely include the migration of both donor T cells and T cell precursors to the thymus to promote central tolerance (15,16,21).

Though chimerism-based strategies for tolerance induction have achieved widespread success in mice, the translation of the intentional induction of stable multilineage mixed chimerism to nonhuman primate (NHP) models and to the clinic has been more challenging. This is especially the case after lower intensity nonmyeloablative pretransplant conditioning, with most work focused on inducing transient chimerism (16,22–26). Alternatively, others have chosen to significantly escalate the intensity of pretransplant conditioning to establish the donor graft (27–30) or to induce full-donor rather than mixed chimerism (31–33). Our group has built on our experience with reduced-intensity pretransplant conditioning and T cell costimulation-blockade-mediated chimerism and tolerance induction in mice (1–3,5,6) as the platform for translation to NHPs. Using an MHC-defined NHP model, we first sought to determine whether we could directly translate the success in mice, using a busulfan-based conditioning regimen and either anti-CD154 or anti-CD40 antibodies plus CD80/CD86-directed costimulation blockade-based immunomodulation, to NHPs. Our previous work demonstrated the successful induction of long-lived (>1 year) myeloid-predominant chimerism with this regimen (1,34–37). However, unlike in mice, reduced-intensity busulfan-only conditioning in NHPs did not lead to significant T cell chimerism (34,35), and without significant T cell chimerism, the donor hematopoietic graft was eventually rejected by host T cells (34,35,38) (at a pace directly related to the degree of MHC disparity) (35). This transient chimerism did not induce tolerance to renal allografts (37). Here, we report an adapted transplant strategy that can lead to long-lived multilineage mixed chimerism, and in the setting of significant T cell chimerism, that is associated with tolerance to donor hematopoiesis and prolonged skin graft acceptance. However, these transplants also provide an important cautionary tale: this tolerance-induction regimen was associated with a significant risk of infectious disease complications (prominently including cytomegalovirus [CMV] reactivation and disease), along with evidence for functional deficits in antiviral protective immunity. Further refinements of this transplant strategy designed to "thread the needle" of allograft tolerance while maintaining intact protective immunity are needed for successful translation to the clinic.

Materials and Methods

Experimental animals

This study used Indian-origin rhesus macaques (18 animals) from the Yerkes National Primate Research Center, the Washington National Primate Research Center and the National Institutes of Health (NIH)-sponsored rhesus macaque colony operated by Alphagenesis Inc. The study was conducted in strict accordance with US Department of Agriculture (USDA) regulations and the recommendations in the *Guide for the Care and Use of Laboratory Animals*. It was approved by both the Emory University and the University of Washington Institutional Animal Care and Use Committees.

MHC typing

Details of the MHC typing and disparity between donors and recipients are described in detail in Supplementary Methods.

Transplant preparation and immunosuppression strategy

The transplant strategy is shown in Figure 1 and is based on our previously published costimulation-blockade-based immunosuppression strategy (34,35), with the addition of low-dose (200 or 300 cGy) total body irradiation (TBI; delivered with a linear accelerator [Varian] at a dose-rate of $\leq$7 cGy/min) to the busulfan-based pretransplant conditioning regimen. Details of the strategy and dosing regimens are described in Supplementary Methods.

Hematopoietic stem cell transplant protocol

Hematopoietic stem cell transplant (HCT) utilized leukopheresis-derived hematopoietic stem cells (HSCs), harvested using a COBE Spectra or Spectra Optia apparatus (Terumo BCT, Inc., Lakewood, CO) from donors that underwent granulocyte colony-stimulating factor (G-CSF)-based mobilization (50 mcg/kg $\times$ 5 days subcutaneously), as previously described (34,35). The total nucleated cell dose/kg, total $CD3^+$ T cell dose/kg and total $CD34^+$ cell dose/kg for each transplant recipient is shown in Table 1.

Chimerism determination

Bone marrow, whole blood and flow-cytometry-sorted myeloid cells ($CD3^-/CD20^-/CD14^+$), T cells ($CD3^+/CD20^-/CD14^-$) and B cells ($CD3^-/CD20^+/CD14^-$) were analyzed for donor chimerism based on divergent microsatellite markers at the UC Davis veterinary genetics laboratory, as previously described (34,35).

CMV monitoring, primary prophylaxis and treatment

CMV monitoring, primary prophylaxis and treatment are described in Supplementary Methods.

ELISPot analysis of CMV-specific T cell immunity

Enzyme-linked immunospot (ELISPot) analysis was performed as previously described and detailed in Supplementary Methods.

Longitudinal flow cytometric analysis of T cell phenotype

Immune cell subpopulations were quantified flow cytometrically as previously described (details supplied in Supplementary Methods).

Skin allografting

Details of skin allografting are supplied in the Supplementary Methods.

Statistical analysis

Analysis of variance (ANOVA) and Kaplan–Meier analysis were carried out using GraphPad Software version 6 (GraphPad, La Jolla, CA). To determine ANOVA for multiple parameters, a *post hoc* Tukey honest significant difference (HST) test was used to determine significant differences for pair-wise comparisons.

Results

Multilineage mixed chimerism in NHPs

In this study we designed a stringent multiyear transplant protocol using MHC-matched transplant pairs

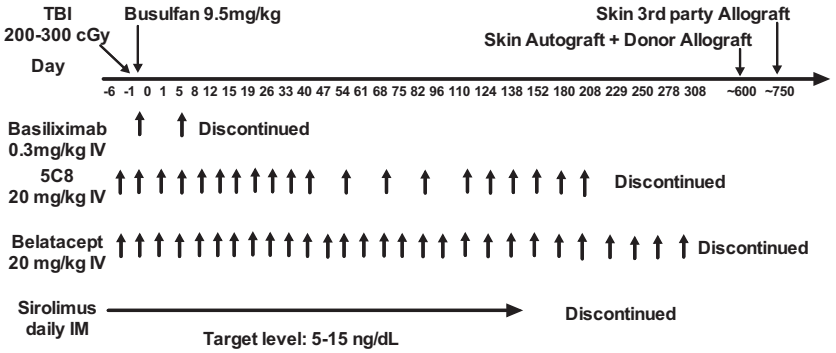

Figure 1: Transplant and immunosuppression strategy. Transplant strategy with details of conditioning regimen, doses of immunosuppression given and immunosuppression discontinuation endpoints. Busulfan was given on day −1 at a dose of 9.5 mg/kg. The hematopoietic stem cell transplant took place on day 0. The immunosuppressive regimen was given as shown by the arrows in the figure, with each arrow representing an individual dose of drug, at the following concentrations: belatacept (20 mg/kg), basiliximab (0.3 mg/kg), anti-CD154 (20 mg/kg), sirolimus (once daily dosing was begun at 0.025 mg/kg and adjusted to achieve a serum trough level of 10–15 mg/mL). Autologous and donor skin grafts were placed as shown. Third-party grafts were placed approximately 150 days after the placement of the donor and autologous skin grafts. TBI, total body irradiation.

Table 1: Transplant and clinical characteristics

Recipient no.	Stem cell source	Total dose of TBI (cGy)	TNC/kg	CD3/kg	CD34/kg	Indication for experiment termination	Infectious disease complications
R.51	PBSC	200	1.4×10^9	9.5×10^7	1.5×10^6	End of experiment	CMV reactivation, pneumonitis
R.52	PBSC	200	1.3×10^9	6.0×10^7	2.6×10^6	End of experiment	CMV reactivation, cellulitis, gingivitis
R.53	PBSC	200	2.9×10^8	2.6×10^6	7.4×10^5	End of experiment	CMV reactivation
R.54	PBSC	200	6.0×10^8	2.1×10^7	3.1×10^6	Weight loss	CMV reactivation
R.55	PBSC	200	4.3×10^8	2.2×10^7	1.1×10^6	Weight loss	CMV reactivation
R.56	PBSC	300	8.4×10^8	3.2×10^7	1.2×10^6	Weight loss	CMV reactivation, *Giardia* enterocolitis
R.57	PBSC	300	6.3×10^8	6.3×10^7	6.2×10^6	CMV colitis	High-level CMV reactivation
R.58	PBSC	300	3.0×10^9	1.2×10^8	6.4×10^6	CMV colitis	High-level CMV reactivation
R.59	PBSC	300	3.0×10^9	5.4×10^8	2.2×10^6	MDR *E. coli* end-organ failure	*Bacillus* bacteremia, MDR *E. coli* bacteremia

CMV, cytomegalovirus; MDR, multi-drug-resistant; PBSC, peripheral blood stem cells; TBI, total body irradiation; TNC, total nucleated cell.

(Table 2), in which our previously published busulfan/costimulation blockade/sirolimus-based regimen (34,35) was modified to enhance donor lymphoid chimerism (39) with low-dose (200–300 cGy) TBI (40–42). As shown in Figure 1, completion of the entire experimental protocol required at least 25 months of follow-up: This included a pretransplant conditioning phase (2 weeks) and on-therapy phase (10 months) during which recipients were first conditioned with nonmyeloablative doses of busulfan + TBI, and then treated with sirolimus/5C8/belatacept, followed by sequential discontinuation in the following order: sirolimus→5C8→belatacept. After all immunosuppression was weaned, recipients were monitored for at least 12 months for chimerism stability, followed by skin allografting. As shown in Figures 2(A) and (B), this conditioning regimen in conjunction with costimulation blockade/sirolimus-based posttransplant immunosuppression was successful in creating multilineage chimerism in all transplant recipients. However, only 3 of the 9 transplanted animals completed the entire transplant protocol; the remaining animals reached protocol endpoint criteria due to clinical evidence of disease not responsive to treatment (on days 32–202 posttransplant), each with infectious toxicities (discussed in detail below). For 2 of the 3 surviving animals, R.51 and R.52, multilineage mixed chimerism was sustained for the entire experiment. For the third transplant recipient, R.53, who received a substandard dose of donor cells after a problematic apheresis procedure (including a ~10-fold lower dose of total nucleated cells [TNCs] CD34+ and CD3+ cells; Table 1), the initial chimerism set point was substantially lower compared with those of the other recipients (27% bone marrow [BM] chimerism at day +30 compared to 88% ± 8.8% in the remaining 8 animals; Figure 2A). As shown in Figure 2(B), R.53 lost chimerism at day 383 posttransplant.

Table 2: Microsatellite-based typing of transplant donors and recipients. Individual MHC haplotypes are color coded

Two MHC-haplotype matched pairs		MHC microsatellites performed at California National Primate Research Center											Non-MHC divergent microsatellite for chimerism testing
Animal ID	Relationship	222I18	MOG-CA	151L13	162B17A	162B17B	246K06	MICA	9P06	DRA-CA	D6S2876	D6S2741	
D.51	Full sibling	167	121	301	250	309	283	200	189	120	203	271	D13S765: 236
D.51	Full sibling	168	123	309	240	293	285	200	191	132	195	269	
R.51	Full sibling	167	121	301	250	309	283	200	189	120	203	271	D13S765: 220
R.51	Full sibling	168	123	309	240	293	285	200	191	132	195	269	
D.52	Half sibling	173	127	305	252	309	285	200	175	126	215	279	D8S1106: 152
D.52	Half sibling	168	123	309	240	297	279	200	191	136	209	261	
R.52	Half sibling	173	127	305	252	309	285	200	175	126	215	279	D8S1106: 144
R.52	Half sibling	168	123	309	240	297	279	200	191	136	209	261	
D.53	Full sibling	167	125	319	242	281	275	194	185	128	0	287	D13S765: 220
D.53	Full sibling	167	121	301	250	309	281	194	187	112	219	269	
R.53	Full sibling	167	125	319	242	281	275	194	185	128	0	287	D13S765: 232
R.53	Full sibling	167	121	301	250	309	281	194	187	112	219	269	
D.54	Full sibling	173	127	305	252	309	283	200	175	126	215	279	D7S513: 207
D.54	Full sibling	168	123	309	240	297	279	200	191	136	209	261	
R.54	Full sibling	173	127	305	252	309	283	200	175	126	215	279	D7S513: 229
R.54	Full sibling	168	123	309	240	297	279	200	191	136	209	261	
D.56	Full sibling	167	125	319	242	281	275	194	185	128	0	287	D3S1768: 221
D.56	Full sibling	167	121	301	250	309	281	194	187	112	219	269	
R.56	Full sibling	167	125	319	242	281	275	194	185	128	0	287	D3S1768: 225
R.56	Full sibling	167	121	301	250	309	281	194	187	112	219	269	
D.57	Full sibling	173	127	305	242	311	277	191	185	134	210	281	D8S1106: 148
D.57	Full sibling	168	123	309	240	297	279	200	191	136	209	261	
R.57	Full sibling	173	127	305	242	311	277	191	185	134	210	281	D8S1106: 160
R.57	Full sibling	168	123	309	240	297	279	200	191	136	209	261	
D.58	Full sibling	173	121	299	240	295	279	200	175	128	219	277	D13S765: 224
D.58	Full sibling	173	127	305	242	293	281	200	175	136	209	277	
R.58	Full sibling	173	121	299	240	295	279	200	175	128	219	277	D13S765: 232
R.58	Full sibling	173	127	305	242	293	281	200	175	136	209	277	
D.59	Full sibling	168	123	321	281	242	275	200	179	128	210	265	D7S513: 217
D.59	Full sibling	167	121	301	289	252	283	200	183	136	209	273	
R.59	Full sibling	168	123	321	281	242	275	200	179	128	210	265	D7S513: 189
R.59	Full sibling	167	121	301	289	252	283	200	183	136	209	273	

Two MHC-haplotype matched pairs		MHC microsatellites performed at Wisconsin National Primate Research Center											Non-MHC divergent microsatellite for chimerism testing
Animal ID	Relationship	D6S2972	D6S2970	D6S2704	D6S2691	193435	MICA	D6S2782	D6S2892	DRA-CA	D6S2876	D6S27345	
D.55	Full sibling	123.6	293.7	153.8	248.6	184.8	204.4	337.5	202.6	233.9	218.8	308.9	D7S513: 299
D.55	Full sibling	119.6	293.7	153.8	284.9	227.6	201.6	337.5	202.6	247.9	195.1	300.5	
R.55	Full sibling	123.6	293.7	153.8	248.7	184.8	204.4	337.6	202.6	234	218.8	309	D7S513: 193
R.55	Full sibling	119.6	293.7	153.8	285	227.7	201.6	337.6	202.6	248	215.1	300.5	

COLOR

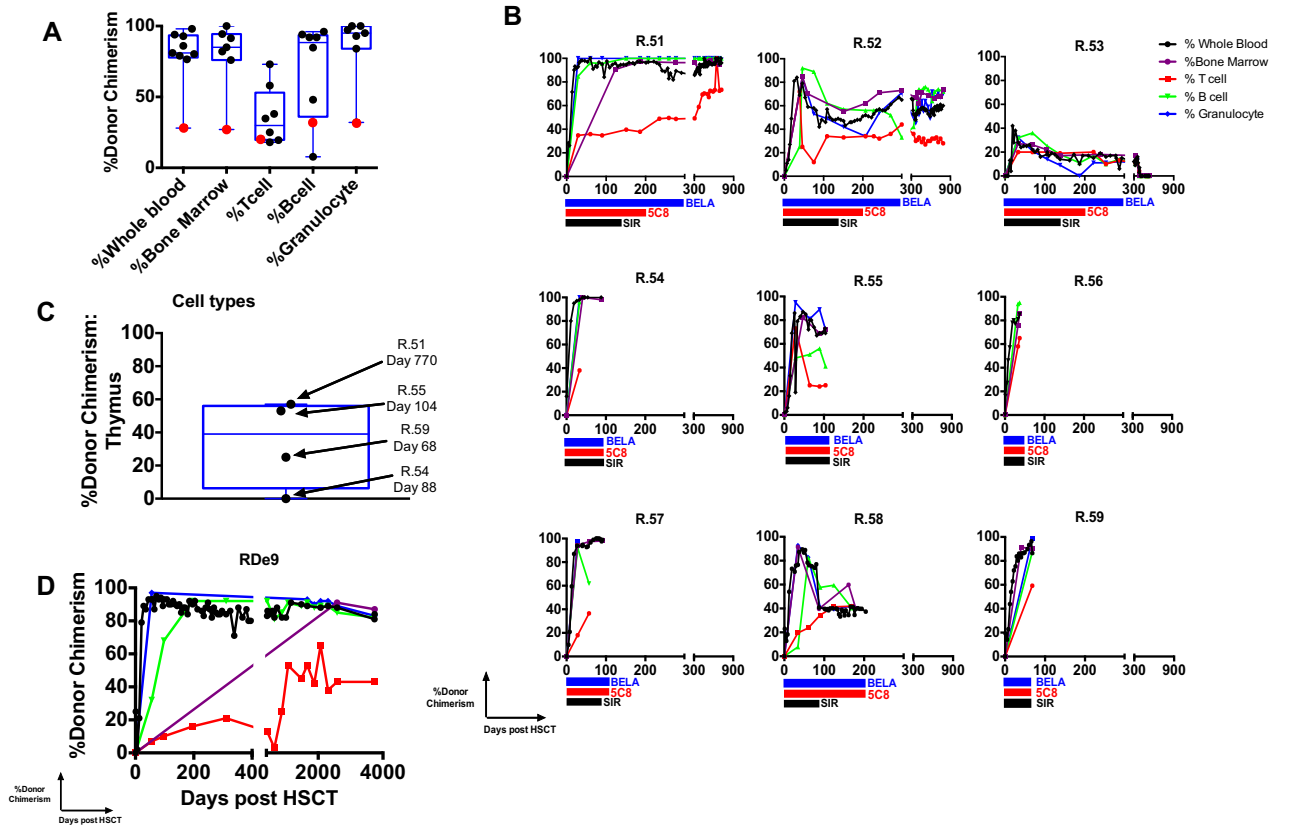

Figure 2: Multilineage mixed chimerism induction after nonmyeloablative HSCT in MHC-matched transplant pairs. (A) Whole blood, bone marrow, T cell, B cell, and granulocyte chimerism of recipient animals at day 30 posttransplant shown as individual points. R.53 is shown as a red point; all other recipients shown as black points. Mean and standard deviation are shown as blue boxes and whiskers. (B) Longitudinal analysis of whole blood chimerism, bone marrow chimerism, T cell chimerism, B cell chimerism, and granulocyte chimerism for all transplant recipients. Color-coded bars below each graph indicate duration of immunosuppression (black bar: sirolimus, "Sir"; red bar: anti-CD154, "5C8"; blue bar: belatacept, "Bela"). (C) Thymic chimerism at time of necropsy for 4 recipients for which thymic tissue was obtainable at necropsy (R.51, R.54, R.55, R59). Individual chimerism values shown as black points. Mean and standard deviation are shown as blue boxes and whiskers. (D) Long-term follow up of whole blood chimerism, bone marrow chimerism, T cell chimerism, B cell chimerism, and granulocyte chimerism for a previously reported (35) recipient (RDe9) with stable multilineage mixed chimerism. HSCT, hematopoietic stem cell transplant.

High incidence of CMV reactivation and other infectious disease complications amid defects in antiviral T cell function

Although the creation of multilineage mixed chimerism that was capable of lasting longer than 2–3 years (Figure 2B) is a striking result, one of the most important observations made in this study was the high incidence of infections that occurred. As shown in Table 1 and Figure 3, transplant recipients all experienced serious infectious disease complications. These prominently included CMV reactivation and disease (despite the fact that all recipients received primary prophylaxis and secondary CMV treatment using a regimen that has successfully prevented high-level CMV reactivation and disease in our other NHP studies) (35) but also included bacterial complications, including *Giardia* enterocolitis, *Bacillus* bacteremia and multi-drug-resistant *Escherichia coli* bacteremia. To quantify the impact of the transplant regimen on T-cell-mediated anti-CMV immunity, we used ELISpot assays (Monkey IFN-γ ELISpot Basic kit from Mabtech, Cincinnati, OH) directed at CMV antigens in 8 animals for which we had available samples. These included 2 transplant recipients who survived long term (R.51 and R.53) and 2 recipients who died early in the setting of CMV reactivation (R.55) and with CMV disease (R.58) (Figure 4). For each transplant, we assayed T cell responses pretransplant for both the recipient and the donor, and at the time of necropsy in the transplant recipient. These results showed significant functional deficits of anti-CMV immunity in R.55 and R.58 at the time of necropsy. In contrast to the results with R.55 and R.58, at the time of necropsy, two of the long-term survivors (R.51 and R.53) had greater CMV-specific responses when compared with their responses at

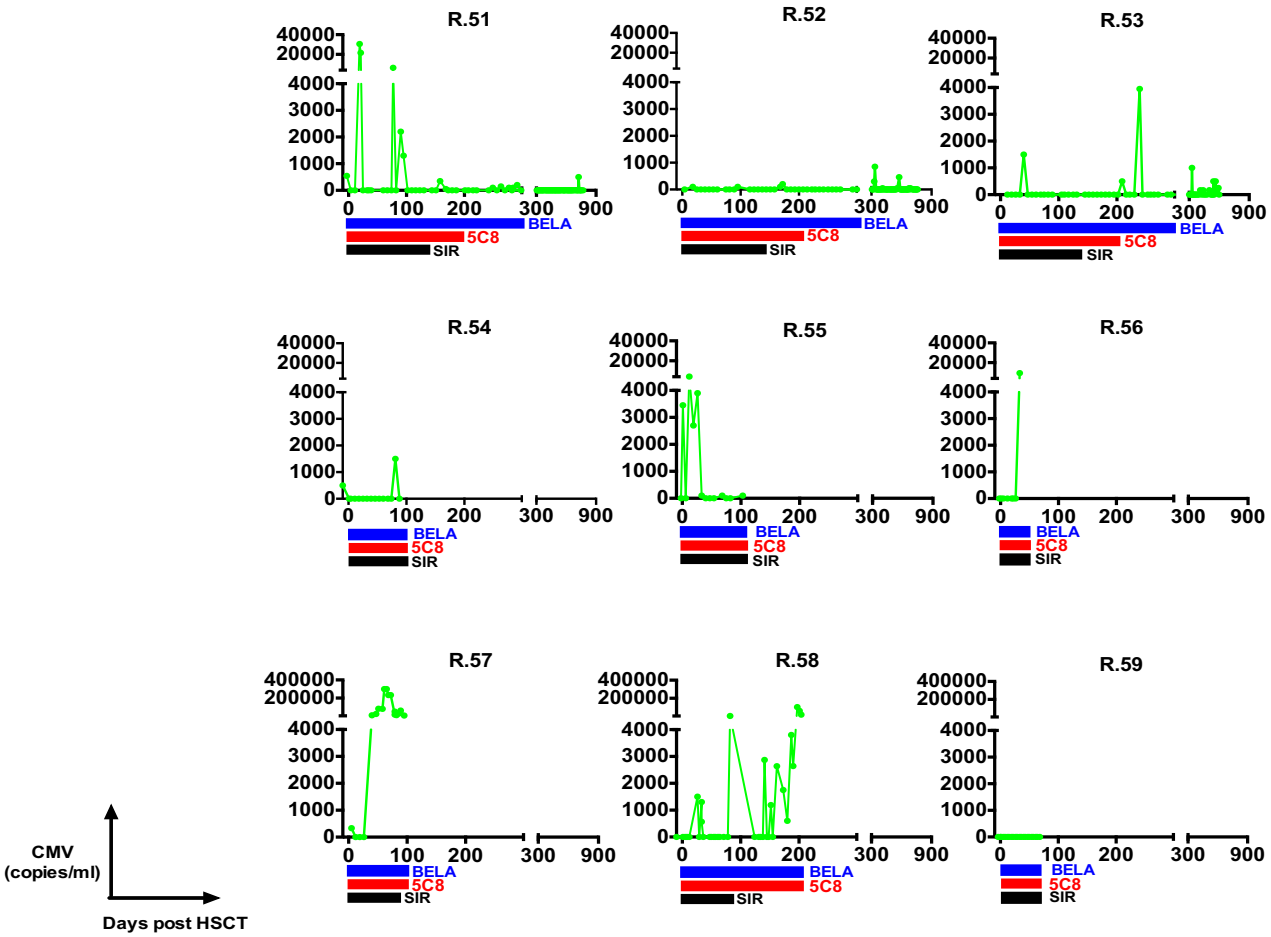

Figure 3: Longitudinal analysis of CMV viral load: CMV viral load is shown for all transplanted animals. Color-coded bars below each graph indicate duration of immunosuppression (black bar: sirolimus, "Sir"; red bar: anti-CD154, "5C8"; blue bar: belatacept, "Bela"). CMV, cytomegalovirus; HSCT, hematopoietic stem cell transplant.

pretransplant. It is important to note that the necropsy samples for the sick animals (R.55 and R.58) were obtained when they were still on immunosuppression, while the necropsy samples from R.51 and R.53 were obtained after immunosuppression withdrawal but with ongoing mixed chimerism.

Impact of sirolimus and costimulation blockade on hematologic reconstitution after transplantation

To investigate the hematologic associations with transplant course, a detailed longitudinal investigation of immune reconstitution was performed. Figure 5 shows the white blood cell (WBC) count, absolute neutrophil count (ANC) and absolute lymphocyte count (ALC) for all recipients. These data demonstrate that generalized lymphopenia developed and persisted in the setting of triple immunosuppression with sirolimus/5C8/belatacept. Whereas the high risk of infectious complications led to early experimental termination in 6 recipients, as noted above, 3 animals (R.51, R.52, and R.53) were evaluable for the entire 25-month experiment. In each of these recipients, lymphopenia persisted after sirolimus withdrawal (during continued costimulation blockade with 5C8 and belatacept) and continued until discontinuation of 5C8, at which time there was a significant increase in lymphocyte counts, despite ongoing treatment with belatacept. There were no further increases in total lymphocyte counts when belatacept was discontinued.

Figure 6 shows a detailed analysis of the impact of immunosuppression withdrawal on B and T cells in R.51. As shown in this figure, as with the total lymphocyte counts (Figure 5), the posttransplant expansion of the T cell compartment was significantly suppressed during triple-agent immunomodulation. Control of T cell expansion persisted despite the discontinuation of sirolimus (in the setting of combined costimulation blockade with 5C8 and belatacept). In contrast, the withdrawal of 5C8 (with continued treatment with belatacept) resulted

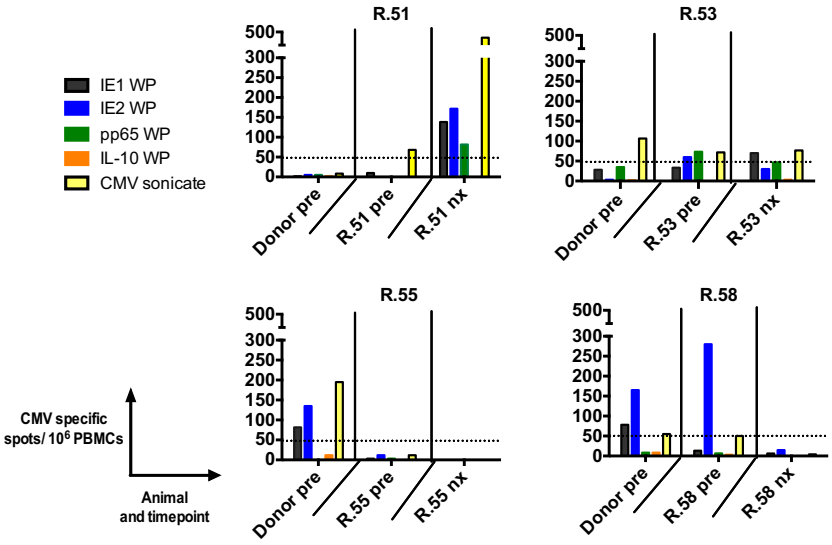

Figure 4: CMV-specific T lymphocyte responses as measured by IFN-γ ELISpot: Responses to whole peptide (WP) pools of rhesus CMV IE1 (black), IE2 (blue), pp65 (green), and IL-10 (orange) and rhesus CMV sonicate (yellow) are shown as spot-forming cells (SFCs) per 1 × 10^6 lymphocytes. Results for 4 evaluable transplant recipients (R.51, R.53, R55, R.58) and their corresponding donors are shown. The threshold for a positive signal with this assay is 50 SFCs/1 × 10^6 lymphocytes (indicated with the dashed line). CMV, cytomegalovirus; PBMCs, peripheral blood mononuclear cells.

in both $CD4^+$ and $CD8^+$ T cell counts significantly rebounding, with no further increase after the discontinuation of belatacept (Figure 6A). The withdrawal of sirolimus and 5C8 also resulted in a significant shift in the T cell subset balance, with a shift in the proportion of both CD4 and CD8 T cell subsets away from the $CD28^+/CD95^-$ naïve phenotype (Figure 6B). In $CD4^+$ T cells, this was accompanied by both a proportional and absolute expansion of $CD28^+/CD95^+$ central memory T cells (Tcm). In CD8+ T cells, the loss of the T-naïve phenotype was accompanied by a significant shift toward both $CD28^+/CD95^+$ Tcm and $CD28^-/CD95^+$ effector memory (Tem) phenotype, with Tcm > Tem expansion. As shown in Figures 6(A) and (B), discontinuation of belatacept and, thus, the total withdrawal of all maintenance immunosuppression resulted in no further shift in subpopulation balance or further expansion of conventional T cell numbers. Analysis of regulatory T cell (Treg) homeostasis demonstrated a different pattern, with a proportional drop in these cells after withdrawal of sirolimus and 5C8, which did not recover until withdrawal of belatacept (Figure 6C). Moreover, the absolute number of Tregs did not significantly expand until after triple immunosuppression withdrawal.

Development of graft-versus-host disease in R.52

Though none of the other animals in this study developed clinically apparent graft-versus-host disease (GVHD), on day 255 posttransplant, animal R.52 developed a skin rash covering 60% of his body surface area (BSA), that, when biopsied, showed histologic evidence of GVHD. This animal had previously experienced an episode of vomiting for which GVHD was considered in the differential diagnosis, but he developed neither diarrhea nor hyperbilirubinemia posttransplant. The diagnosis of GVHD prompted us to treat this recipient with oral prednisone from day 271 to day 550 posttransplant (with weaning and full discontinuation of prednisone prior to skin graft placement). Of note, T cell chimerism was stable prior to, during and after the development and treatment of R.52 for GVHD (see Figure 2B).

Prolongation of donor skin graft acceptance in transplant recipients with significant T cell chimerism

The survival of R.51, R.52, and R.53 to the 2+ year experimental endpoint allowed us to test the impact of T cell chimerism on skin graft survival. We had tested this on a previously reported animal (RQq9, conditioned with busulfan alone, without concomitant TBI), who had developed very low T cell chimerism and who had demonstrated donor skin graft rejection within 30 days (35). As shown in Figure 7, in the current study, we observed a direct relationship between the percent T cell chimerism and the length of skin allograft survival. Thus, as shown in Figure 7(A), R.51, who demonstrated stable, high-level T cell chimerism (~70% at the time of skin-graft placement), demonstrated long-term acceptance of both autologous and donor skin (>100 days) despite rapid rejection of unrelated, third-party skin (rejection by 9 days post-skin-graft placement; Figure 7A). R.51 is thus the first NHP in our experience to meet the formal definition of long-term stable multilineage mixed-chimerism and donor-specific tolerance, having maintained

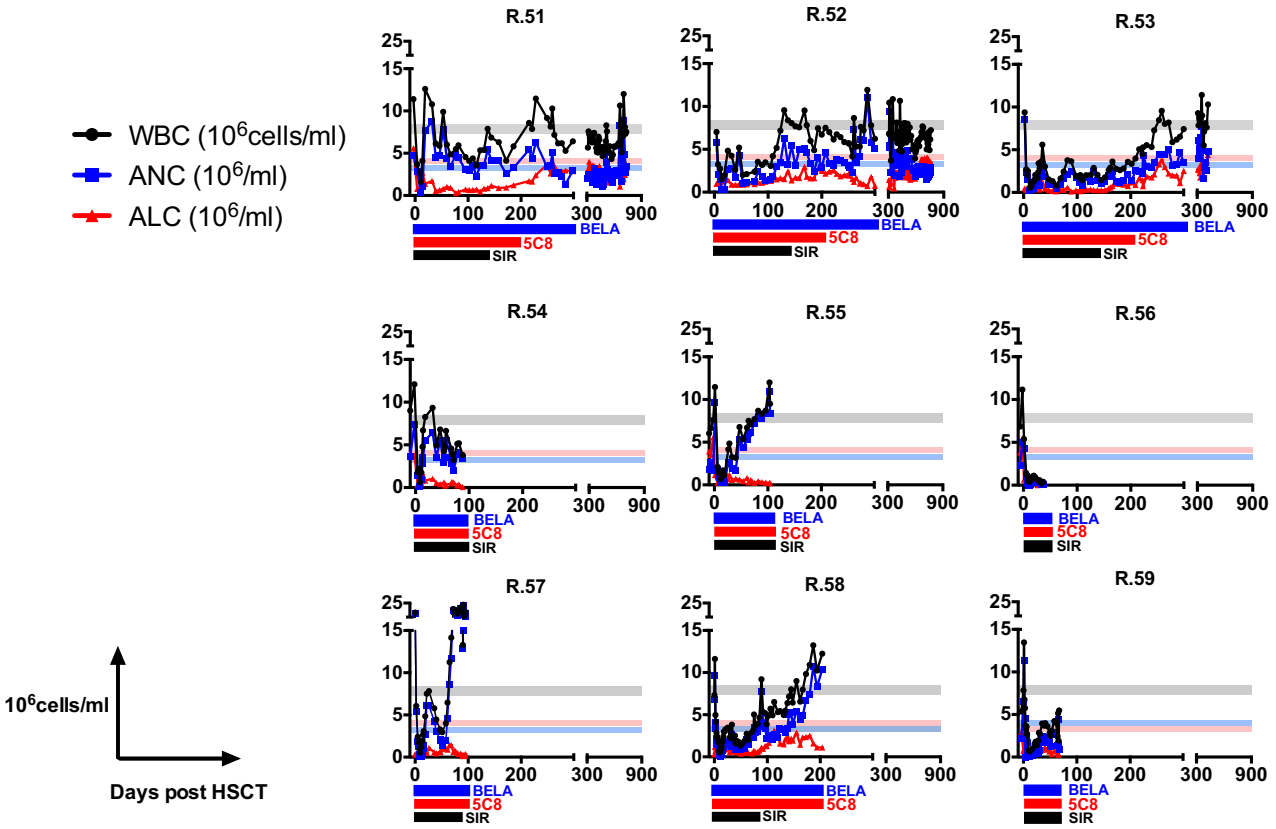

Figure 5: Longitudinal analysis of hematologic reconstitution after transplant. Shown are the white blood cell count (WBCs = black circles), absolute neutrophil count (ANC = blue squares) and absolute lymphocyte count (ALC = red triangles). Color-coded bars below each graph indicate duration of immunosuppression (black bar: sirolimus, "Sir"; red bar: anti-CD154, "5C8"; blue bar: belatacept, "Bela"). Normal values are shown in the graph (mean ±SEM) for WBC (gray bar), ANC (red bar), ALC (blue bar). HSCT, hematopoietic stem cell transplant.

mixed donor-recipient hematopoiesis for over 700 days and donor-specific acceptance of skin allografts for over 100 days.

R.52, who demonstrated significant levels of T cell chimerism, but at levels lower than in R.51, also demonstrated significant prolongation of donor skin graft acceptance. In this recipient, third-party skin was rejected promptly (9 days), and donor skin was accepted for significantly longer (~69 days; Figure 7B). Importantly, however, R.52 eventually rejected the donor skin, and autologous skin was accepted long term. It should be noted, as discussed above, that R.52 was also the animal who developed skin GVHD.

Recipient R.53, who lost donor chimerism prior to skin graft placement, showed rejection of the donor skin graft at a similar tempo to previous recipients who had never developed T cell chimerism, showing signs of rejection by day 40 post-skin-graft placement (Figure 7C). This observation is important because it provides evidence to support the hypothesis that significant T cell chimerism, rather than the conditioning regimen (which was identical in R.51, R.52, and R.53), was associated with skin graft tolerance.

Of note, a fourth recipient, RDe9, who had been previously reported as the one recipient with stable chimerism in an earlier experimental cohort not receiving TBI (35) (for whom the donor was unfortunately not available for skin grafting) has now been followed for more than 10 years posttransplant and has been a stable multilineage mixed chimera for the entire follow-up period, in the setting of substantial T cell chimerism (currently at 30%, with follow-up for >10 years; Figure 2D). Taken together, these results are consistent with the acquisition of T cell chimerism as highly associated with long-term allograft acceptance, including both acceptance of bone marrow and skin graft tolerance.

Indeed, although the number of recipients analyzed was small, three important observations arise from the skin allograft experiments, shown in Figure 7. First, we found that it was possible to create a scenario (R.51) in which tolerance to both bone marrow and skin was created.

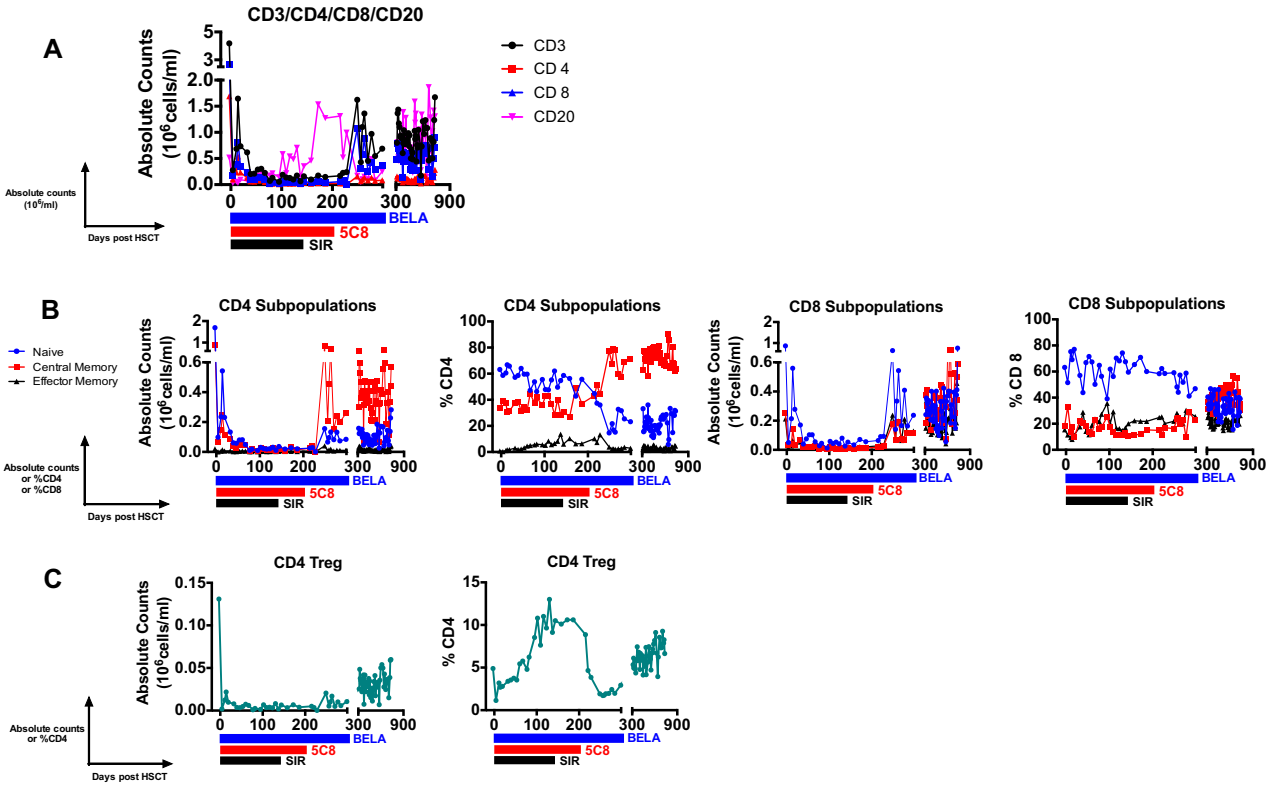

Figure 6: Immunophenotypic analysis of T cell subset balance after transplant in R.51. (A) Longitudinal analysis of R.51 showing the absolute number of CD3+/CD20– T cells, CD3–/CD20+ B cells, CD3+/CD20–/CD4+/CD8– T cells, and CD3+/CD20–/CD4–/CD8+ T cells in R.51. Black circles: CD3+ T cells. Pink upside triangles: CD20+ B cells. Red squares: CD4+ T cells. Blue triangles: CD8+ T cells. X axis: Day posttransplant. Y axis: Absolute cell counts. Color-coded bars below each graph indicate duration of immunosuppression (black bar: sirolimus, "Sir"; red bar: anti-CD154, "5C8"; blue bar: belatacept, "Bela"). (B) Longitudinal analysis of R.51 showing absolute numbers and relative % of either CD4+ or CD8+ T cell subsets, defined as follows: naïve (CD28+/CD95–; blue circles), central memory (CD28+/CD95+; red squares) and effector memory (CD28–/CD95+; black triangles). X axis: Day posttransplant. Y axis: Absolute cell counts or % of CD4+ or CD8+ T cells. Color-coded bars below each graph indicate duration of immunosuppression (black bar: sirolimus, "Sir"; red bar: anti-CD154, "5C8"; blue bar: belatacept, "Bela"). (C) Longitudinal analysis of R.51 showing absolute numbers and % of CD4+ T cells of CD4+/CD3+/FoxP3+/CD25+ Tregs. X axis: Days posttransplant. Y axis: Absolute cell count or % Tregs of total CD4+ T cells. Color-coded bars below each graph indicate duration of immunosuppression (black bar: sirolimus, "Sir"; red bar: anti-CD154, "5C8"; blue bar: belatacept, "Bela"). HSCT, hematopoietic stem cell transplant; Treg, regulatory T cells.

Second, in the 4 animals on whom skin grafts were placed (3 in the current study, 1 in a previous study [35]), there was a direct correlation between the percent T cell chimerism and donor allograft survival (Figure 7D). Finally, in each of these animals, immune competence to allografts were maintained, given the rapid rejection of third-party skin in 3/3 animals tested.

Discussion

In this study, we demonstrate that a transplant strategy employing a nonmyeloablative busulfan/TBI conditioning regimen and costimulation blockade plus sirolimus-based immunomodulation can reliably produce multilineage mixed chimerism, and in the setting of substantial and stable T cell chimerism, donor-specific acceptance of a skin allograft is achievable. These results are notable, given the demonstration that stable multilineage mixed chimerism can be intentionally created in primates. This represents, to our knowledge, the longest duration of stable multilineage mixed chimerism induction in NHPs. As such, these data provide proof-of-concept that, even in outbred primates, stable T cell mixed chimerism can be achieved by design. As we will discuss in detail below, the results of this study also underscore the significant risks of infectious disease complications that can accompany this transplant regimen, indicating that further modifications are necessary before translation to the clinic.

This study is distinguished from others in the field by two facts: (1) It sought to intentionally create *mixed donor/recipient T cell chimerism,* and (2) it sought to

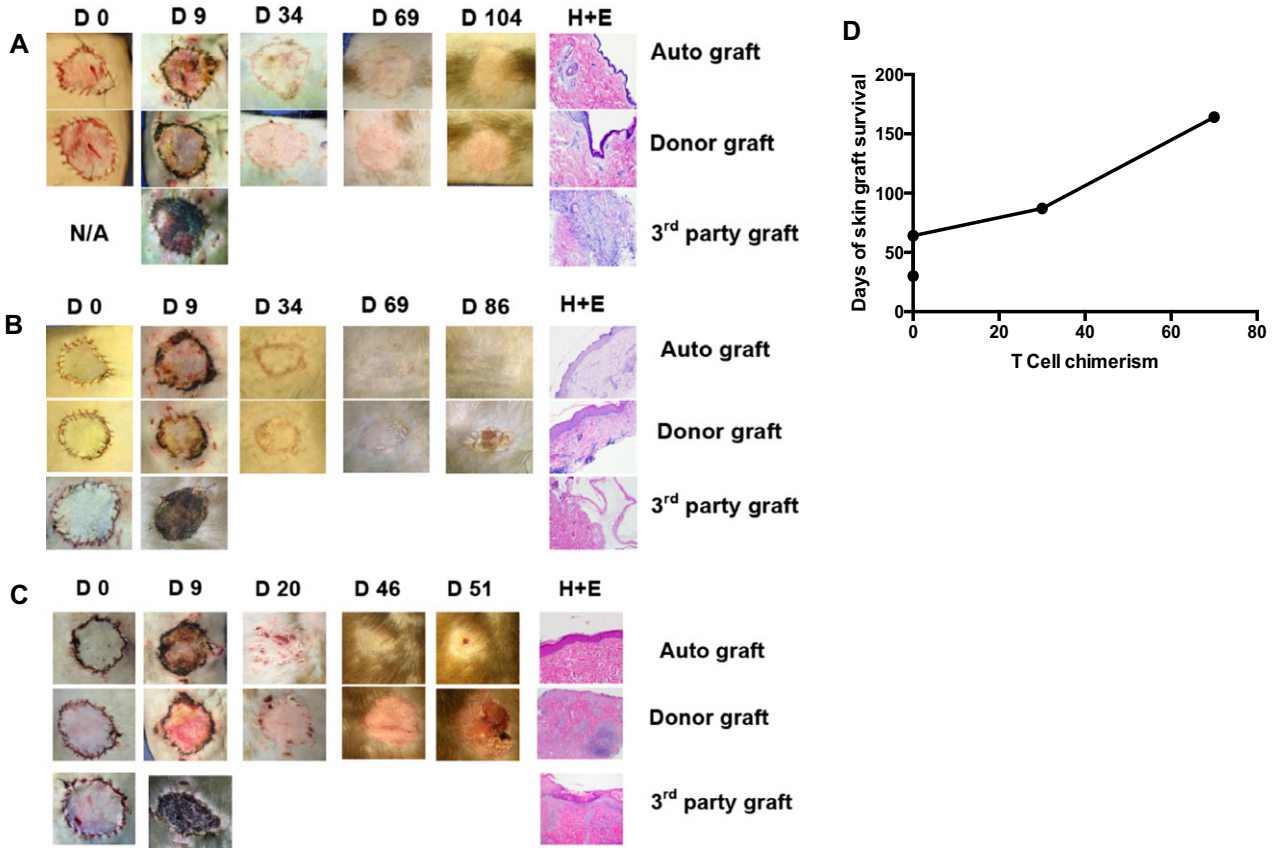

Figure 7: Skin grafting in long-term surviving transplant recipients, showing autologous skin grafts, donor skin grafts, and nonrecipient, nondonor "third-party" skin grafts. (A) R.51: Representative photographs of autologous, donor, and third-party skin grafts at days 0, 9, 34, 69, and 104 after graft placement. To the right of each graft, representative hemotoxylin and eosin (H&E) staining is shown, documenting lymphocyte infiltration of the third-party graft without infiltration of either the autologous or donor skin grafts. (B) R.52: Representative photographs of autologous, donor and third-party skin grafts at days 0, 9, 34, 69 and 86 after graft placement. Right column: Representative H&E staining of the autologous graft showing no lymphocytic infiltration, representative H&E staining of the donor graft showing lymphocytic infiltration and representative H&E staining of the third-party allograft with eschar formation postrejection. (C) R.53: Representative photographs of autologous, donor and third-party skin grafts at days 0, 9, 20, 46, and 51 after graft placement. Right column: Representative H&E staining of the autologous graft showing no lymphocytic infiltration, representative H&E staining of the donor graft showing lymphocytic infiltration and representative H&E staining of the third-party allograft with eschar formation postrejection. (D) Graph showing the relationship between the % T cell chimerism (y axis) and donor skin graft acceptance (x axis). Data are from R.51, R.52 and R.53 from the current study and for a previously reported (35) recipient (RQq9).

create multilineage mixed chimerism that was *stable posttransplant*. Thus, the group at Massachusetts General Hospital (MGH) has developed a transplant regimen in NHPs that leads to transient donor chimerism, with rejection of the donor bone marrow transplant (BMT) within 1 month of transplantation (22–26). In NHPs, this regimen is effective in achieving long-term renal allograft tolerance in approximately half of the renal transplant recipients. Encouragingly, clinical trials of BMT plus renal transplant based on these NHP studies resulted in multiple patients being weaned off of immunosuppression (27,28,43–45). However, a significant engraftment syndrome (43) developed in several patients, suggesting that loss of the donor hematopoietic graft may have untoward effects in humans that were not observed in NHPs.

An independent clinical transplant series from the Stanford group has led to sustained donor chimerism in the setting of intensive total lymphoid irradiation (TLI; 1200 cGy) plus anti-thymocyte globulin (ATG) during combined BMT plus renal transplant. This regimen has been successful in achieving stable mixed chimerism and tolerance to the renal allograft in a number of MHC-matched donor/recipient pairs (27–30). Whether this regimen will be translatable to the more commonly encountered MHC-mismatched setting is not yet known. Finally, the Leventhal and Ildstadt group has reported full donor engraftment (ie not *mixed* chimerism, but rather full replacement with donor hematopoieisis) and long-term allograft acceptance in patients given combined hematopoietic and renal transplants in the presence of

facilitating cells. Though this trial is not a "mixed-chimerism" trial per se, if long-term GVHD-free immunosuppression-free survival becomes a reality for these patients, it is of high significance to the field.

In the current study, by closely monitoring the impact of sequential withdrawal of sirolimus, followed by anti-CD154, followed by belatacept, we gained important insights into the impact of triple, dual and single immunomodulation on T cell reconstitution and subpopulation balance. Our results demonstrate a significant suppression of absolute T cell counts and preservation of naïve T cell predominance during sirolimus and dual costimulation blockade. The suppression of T cell expansion and changes in T cell subpopulation balance were maintained despite discontinuation of sirolimus. When anti-CD154 treatment was also discontinued (during monotherapy treatment with belatacept), we observed both T cell expansion and a shift in the subpopulation balance, from a Tnaive predominance to a Tcm predominance for both CD4 and CD8 T cells (with CD8 T cells also expanding the Tem compartment). Importantly, although no further quantitative or qualitative changes occurred in the conventional T cell compartment after withdrawal of belatacept, discontinuation of this therapy was associated with expansion of Tregs. The shift in CD8+ T cells to a Tcm (rather than a Tem) predominance is a new finding that we have not observed with our previous mixed-chimerism experiments (34–37). Although this, along with the eventual expansion of Tregs is notable, it is not clear whether these shifts represent causation or correlation with tolerance induction. As such, this represents an important area for future study. Importantly, these data also indicate that reciprocal tolerance to both donor and recipient hematopoiesis could persist despite both the T cell expansion and the shift in the naïve/memory T cell balance that occurred after immunosuppression withdrawal, indicating robust control of both host-versus-graft and graft-versus-host vectors of T cell activation toward hematopoiesis with this transplant strategy.

The stability of bidirectional tolerance to hematopoiesis (permitting the coexistence of both donor and recipient T cells) also suggests that central tolerance mechanisms contributed to long-term acceptance of the hematopoietic graft in this model. The observation of donor chimerism in 3 of 4 isolated thymi is supportive of this hypothesis (Figure 2C). The significant duration of triple→double→single agent immunomodulation (with some form of immunosuppression present for 300 days posttransplant) may have facilitated the development of central tolerance, by providing sufficient immunosuppression-mediated immune restraint to permit trafficking of donor cells to the thymus.

One of the other central experiments performed in this transplant series was the placement of autologous, donor and nondonor "third-party" skin allografts a full year after withdrawal of sirolimus and costimulation blockade. This experiment demonstrated long-term acceptance (>100 days) in the recipient with the highest level of T cell chimerism, prolonged but limited skin graft acceptance in a recipient with lower but still significant T cell tolerance and prompt rejection of donor skin in two recipients with no T cell chimerism. These data suggest that, as in mice, in primates tolerance to tissues may require significant, stable T cell chimerism. One important caveat to the current studies is the well-recognized "high bar" for tolerance induction that skin grafts represent. It is possible that less immunogenic grafts, such as renal or liver allografts, could have a lower threshold for T cell chimerism required for tolerance induction. Indeed, we also observed GVHD of the skin in R.52, which, though reversible with steroids, suggests that the difficulty in attaining tolerance to skin antigens occurred in both the host-versus-graft and the graft-versus-host directions in this animal. Renal allograft studies (both proof-of-concept delayed renal transplantation as well as renal allografts placed concurrently with chimerism induction) thus represent an important area for future research, once an optimized regimen, able to support stable mixed chimerism while minimizing infectious complications, is developed.

Despite the success in creating donor chimerism that was capable of lasting for several years, the extremely high rate of loss of our transplant recipients due to infectious disease complications represents a sobering reality. In the current study, 8/9 recipients experienced CMV reactivation, despite all recipients receiving primary prophylaxis with cidofovir. In 2 of these recipients, CMV end-organ disease was associated with recipient death, underscoring the seriousness of CMV disease in this transplant regimen and the difficulty of reversing CMV disease in NHPs, a phenomenon that has been documented previously by our group and others (34,35,46–51). Whether the clinical challenges encountered with this virus are an inherent attribute of the NHP-specific CMV virus or due to decreased efficacy of standard antivirals against rhesus CMV is not known. Delivering effective treatment for CMV is also considerably more challenging in NHPs than in patients, which could also have negatively affected our ability to control reactivated virus. Importantly, the most significant infectious disease complications occurred during the period of active immunosuppression, rather than during the period of sustained mixed chimerism, with R.52 and R.53 being much more stable from an infectious disease standpoint after immunosuppression withdrawal than they were on triple-, double-, or single-agent therapy. This observation suggests that a rigorous step-wise elimination experiment is warranted to determine which elements of the conditioning regimen and immunomodulatory strategy are required for stable multilineage mixed chimerism and which produce the most severe functional defects in

protective immunity. If successful, this approach may yield a regimen that can succeed in producing tolerance without the defects in protective immunity observed in this transplant series. Although it is not yet clear which of the elements of pretransplant conditioning or post-transplant immunomodulation are the most important to eliminate or alter, our results suggest that a regimen that drives less severe lymphopenia while maintaining a positive Treg:Tcon balance would potentially tip the balance in favor of specific tolerance to the donor with less global defects in antiviral protective immunity.

In summary, this transplant series has demonstrated a series of important milestones as well as challenges to tolerance induction. We describe a transplant regimen that is consistently able to induce multilineage mixed chimerism as well as proof-of-concept that in the setting of significant T cell mixed chimerism, donor-specific tolerance, even to a highly immunogenic skin graft, is possible. We also demonstrate an important pitfall with this regimen, encapsulated by the significant clinical risks of infectious disease-related morbidity and mortality that these transplant recipients faced. These risks provide strong rationale for further iteration of this tolerance induction strategy to identify the minimally effective immunomodulation strategy. Standing at the precipice of intentional multilineage mixed chimerism and tolerance induction, these studies underscore both the significant benefits that these approaches may represent to patients as well as the risks, and they emphasize the precision with which clinically successful regimens will need to be formulated.

Acknowledgments

This work was funded by NIH NIAID 5U19-AI051731 (L.S.K., C.P.L., A.B.A., A.D.K.), NIH NHLBI 5 R01 HL095791 (L.S.K.) and P01 AI056299 (B.R.B.). We gratefully acknowledge the work of Dr. Cecelia Penedo and Ms. Thea Ward of the California National Primate Research Center as well as Dr. Roger Wiseman and Dr. David O'Connor, who performed microsatellite-based MHC typing and chimerism analysis for this study. We thank the veterinary staff of both the Yerkes National Primate Research Center and the Washington National Primate Research Center for their expert veterinary assistance with these studies.

Disclosure

The authors of this manuscript have no conflicts of interest to disclose as described by the *American Journal of Transplantation*.

References

1. Adams AB, Durham MM, Kean L, et al. Costimulation blockade, busulfan, and bone marrow promote titratable macrochimerism, induce transplantation tolerance, and correct genetic hemoglobinopathies with minimal myelosuppression. J Immunol 2001; 167: 1103–1111.
2. Corbascio M, Ekstrand H, Osterholm C, et al. CTLA4Ig combined with anti-LFA-1 prolongs cardiac allograft survival indefinitely. Transpl Immunol 2002; 10: 55–61.
3. Durham MM, Bingaman AW, Adams AB, et al. Cutting edge: Administration of anti-CD40 ligand and donor bone marrow leads to hemopoietic chimerism and donor-specific tolerance without cytoreductive conditioning. J Immunol 2000; 165: 1–4.
4. Ildstad ST, Wren SM, Bluestone JA, Barbieri SA, Sachs DH. Characterization of mixed allogeneic chimeras. Immunocompetence, *in vitro* reactivity, and genetic specificity of tolerance. J Exp Med 1985; 162: 231–244.
5. Kean LS, Durham MM, Adams AB, et al. A cure for murine sickle cell disease through stable mixed chimerism and tolerance induction after nonmyeloablative conditioning and major histocompatibility complex-mismatched bone marrow transplantation. Blood 2002; 99: 1840–1849.
6. Larsen CP, Elwood ET, Alexander DZ, et al. Long-term acceptance of skin and cardiac allografts after blocking CD40 and CD28 pathways. Nature 1996; 381: 434–438.
7. Sykes M. Hematopoietic cell transplantation for the induction of allo- and xenotolerance. Clin Transplant 1996; 10: 357–363.
8. Sykes M, Szot GL, Swenson KA, Pearson DA. Induction of high levels of allogeneic hematopoietic reconstitution and donor-specific tolerance without myelosuppressive conditioning. Nat Med 1997; 3: 783–787.
9. Tomita Y, Khan A, Sykes M. Role of intrathymic clonal deletion and peripheral anergy in transplantation tolerance induced by bone marrow transplantation in mice conditioned with a nonmyeloablative regimen. J Immunol 1994; 153: 1087–1098.
10. Tomita Y, Khan A, Sykes M. Mechanism by which additional monoclonal antibody (mAB) injections overcome the requirement for thymic irradiation to achieve mixed chimerism in mice receiving bone marrow transplantation after conditioning with anti-T cell mABs and 3-Gy whole body irradiation. Transplantation 1996; 61: 477–485.
11. Wekerle T, Blaha P, Koporc Z, Bigenzahn S, Pusch M, Muehlbacher F. Mechanisms of tolerance induction through the transplantation of donor hematopoietic stem cells: Central versus peripheral tolerance. Transplantation 2003; 75(9 Suppl): 21S–25S.
12. Wekerle T, Kurtz J, Ito H, et al. Allogeneic bone marrow transplantation with co-stimulatory blockade induces macrochimerism and tolerance without cytoreductive host treatment. Nat Med 2000; 6: 464–469.
13. Wekerle T, Kurtz J, Sayegh M, et al. Peripheral deletion after bone marrow transplantation with costimulatory blockade has features of both activation-induced cell death and passive cell death. J Immunol 2001; 166: 2311–2316.
14. Wekerle T, Sayegh MH, Hill J, et al. Extrathymic T cell deletion and allogeneic stem cell engraftment induced with costimulatory blockade is followed by central T cell tolerance. J Exp Med 1998; 187: 2037–2044.
15. Umemura A, Morita H, Li XC, Tahan S, Monaco AP, Maki T. Dissociation of hemopoietic chimerism and allograft tolerance after allogeneic bone marrow transplantation. J Immunol 2001; 167: 3043–3048.
16. Nikolic B, Khan A, Sykes M. Induction of tolerance by mixed chimerism with nonmyeloblative host conditioning: The importance of overcoming intrathymic alloresistance. Biol Blood Marrow Transplant 2001; 7: 144–153.

17. Andreani M, Testi M, Battarra M, et al. Relationship between mixed chimerism and rejection after bone marrow transplantation in thalassaemia. Blood Transfus 2008; 6: 143–149.
18. Hsieh MM, Fitzhugh CD, Tisdale JF. Allogeneic hematopoietic stem cell transplantation for sickle cell disease: The time is now. Blood 2011; 118: 1197–1207.
19. Hsieh MM, Kang EM, Fitzhugh CD, et al. Allogeneic hematopoietic stem-cell transplantation for sickle cell disease. N Engl J Med 2009; 361: 2309–2317.
20. Ozyurek E, Cowan MJ, Koerper MA, Baxter-Lowe LA, Dvorak CC, Horn BN. Increasing mixed chimerism and the risk of graft loss in children undergoing allogeneic hematopoietic stem cell transplantation for non-malignant disorders. Bone Marrow Transplant 2008; 42: 83–91.
21. Pilat N, Wekerle T. Transplantation tolerance through mixed chimerism. Nat Rev Nephrol 2010; 6: 594–605.
22. Kawai T, Abrahamian G, Sogawa H, et al. Costimulatory blockade for induction of mixed chimerism and renal allograft tolerance in nonhuman primates. Transplant Proc 2001; 33: 221–222.
23. Kawai T, Cosimi AB, Colvin RB, et al. Mixed allogeneic chimerism and renal allograft tolerance in cynomolgus monkeys. Transplantation 1995; 59: 256–262.
24. Kawai T, Sogawa H, Boskovic S, et al. CD154 blockade for induction of mixed chimerism and prolonged renal allograft survival in nonhuman primates. Am J Transplant 2004; 4: 1391–1398.
25. Kimikawa M, Kawai T, Sachs DH, Colvin RB, Bartholomew A, Cosimi AB. Mixed chimerism and transplantation tolerance induced by a nonlethal preparative regimen in cynomolgus monkeys. Transplant Proc 1997; 29: 1218.
26. Kimikawa M, Sachs DH, Colvin RB, Bartholomew A, Kawai T, Cosimi AB. Modifications of the conditioning regimen for achieving mixed chimerism and donor-specific tolerance in cynomolgus monkeys. Transplantation 1997; 64: 709–716.
27. Scandling JD, Busque S, Dejbakhsh-Jones S, et al. Tolerance and chimerism after renal and hematopoietic-cell transplantation. N Engl J Med 2008; 358: 362–368.
28. Scandling JD, Busque S, Shizuru JA, Engleman EG, Strober S. Induced immune tolerance for kidney transplantation. N Engl J Med 2011; 365: 1359–1360.
29. Strober S, Spitzer TR, Lowsky R, Sykes M. Translational studies in hematopoietic cell transplantation: Treatment of hematologic malignancies as a stepping stone to tolerance induction. Semin Immunol 2011; 23: 273–281.
30. Levin B, Hoppe RT, Collins G, et al. Treatment of cadaveric renal transplant recipients with total lymphoid irradiation, antithymocyte globulin, and low-dose prednisone. Lancet 1985; 2: 1321–1325.
31. Leventhal JR, Elliott MJ, Yolcu ES, et al. Immune reconstitution/immunocompetence in recipients of kidney plus hematopoietic stem/facilitating cell transplants. Transplantation 2015; 99: 288–298.
32. Leventhal J, Abecassis M, Miller J, et al. Chimerism and tolerance without GVHD or engraftment syndrome in HLA-mismatched combined kidney and hematopoietic stem cell transplantation. Sci Transl Med 2012; 4: 124ra28.
33. Leventhal J, Abecassis M, Miller J, et al. Tolerance induction in HLA disparate living donor kidney transplantation by donor stem cell infusion: Durable chimerism predicts outcome. Transplantation 2013; 95: 169–176.
34. Kean LS, Adams AB, Strobert E, et al. Induction of chimerism in rhesus macaques through stem cell transplant and costimulation blockade-based immunosuppression. Am J Transplant 2007; 7: 320–335.
35. Larsen CP, Page A, Linzie KH, et al. An MHC-defined primate model reveals significant rejection of bone marrow after mixed chimerism induction despite full MHC matching. Am J Transplant 2010; 10: 2396–2409.
36. Page A, Srinivasan S, Singh K, et al. CD40 blockade combines with CTLA4Ig and sirolimus to produce mixed chimerism in an MHC-defined rhesus macaque transplant model. Am J Transplant 2012; 12: 115–125.
37. Ramakrishnan SK, Page A, Farris AB 3rd, et al. Evidence for kidney rejection after combined bone marrow and renal transplantation despite ongoing whole-blood chimerism in rhesus macaques. Am J Transplant 2012; 12: 1755–1764.
38. Page A, Srinivasan S, Singh K, et al. CD40 blockade combines with CTLA4Ig and sirolimus to produce mixed chimerism in an MHC-defined rhesus macaque transplant model. Am J Transplant 2011; doi: 10.1111/j.1600-6143.2011.03737.x. [Epub ahead of print].
39. Ishii E, Gengozian N, Good RA. Influence of dimethyl myleran on tolerance induction and immune function in major histocompatibility complex-haploidentical murine bone-marrow transplantation. Proc Natl Acad Sci USA 1991; 88: 8435–8439.
40. Laport GG, Sandmaier BM, Storer BE, et al. Reduced-intensity conditioning followed by allogeneic hematopoietic cell transplantation for adult patients with myelodysplastic syndrome and myeloproliferative disorders. Biol Blood Marrow Transplant 2008; 14: 246–255.
41. Maris M, Storb R. The transplantation of hematopoietic stem cells after non-myeloablative conditioning: A cellular therapeutic approach to hematologic and genetic diseases. Immunol Res 2003; 28: 13–24.
42. McSweeney PA, Niederwieser D, Shizuru JA, et al. Hematopoietic cell transplantation in older patients with hematologic malignancies: Replacing high-dose cytotoxic therapy with graft-versus-tumor effects. Blood 2001; 97: 3390–3400.
43. Farris AB, Taheri D, Kawai T, et al. Acute renal endothelial injury during marrow recovery in a cohort of combined kidney and bone marrow allografts. Am J Transplant 2011; 11: 1464–1477.
44. Kawai T, Cosimi AB, Spitzer TR, et al. HLA-mismatched renal transplantation without maintenance immunosuppression. N Engl J Med 2008; 358: 353–361.
45. LoCascio SA, Morokata T, Chittenden M, et al. Mixed chimerism, lymphocyte recovery, and evidence for early donor-specific unresponsiveness in patients receiving combined kidney and bone marrow transplantation to induce tolerance. Transplantation 2010; 90: 1607–1615.
46. Lo DJ, Anderson DJ, Weaver TA, et al. Belatacept and sirolimus prolong nonhuman primate renal allograft survival without a requirement for memory T cell depletion. Am J Transplant 2013; 13: 320–328.
47. Lowe MC, Badell IR, Turner AP, et al. Belatacept and sirolimus prolong nonhuman primate islet allograft survival: Adverse consequences of concomitant alefacept therapy. Am J Transplant 2013; 13: 312–319.
48. Barry AP, Silvestri G, Safrit JT, et al. Depletion of CD8+ cells in sooty mangabey monkeys naturally infected with simian immunodeficiency virus reveals limited role for immune control of virus replication in a natural host species. J Immunol 2007; 178: 8002–8012.
49. Kaur A, Kassis N, Hale CL, et al. Direct relationship between suppression of virus-specific immunity and emergence of

cytomegalovirus disease in simian AIDS. J Virol 2003; 77: 5749–5758.
50. Kaur A, Hale CL, Noren B, Kassis N, Simon MA, Johnson RP. Decreased frequency of cytomegalovirus (CMV)-specific CD4+ T lymphocytes in simian immunodeficiency virus-infected rhesus macaques: Inverse relationship with CMV viremia. J Virol 2002; 76: 3646–3658.
51. Fiala M, Mosca JD, Barry P, Luciw PA, Vinters HV. Multi-step pathogenesis of AIDS—Role of cytomegalovirus. Res Immunol 1991; 142: 87–95.

Supporting Information

Additional Supporting Information may be found in the online version of this article.

Data S1: Supplementary methods.